Geologia Croatica
Journal of the Croatian Geological Survey and the Croatian Geological Society
2022 | 75/Special Issue | 303–315 | 9 Figs. | 5 Tabs. | www.geologia-croatica.hr

Trace elements in pyrite from the Čukaru Peki porphyry Cu-high-sulfidation deposit, Serbia: implications for ore evolution in a polyphase hydrothermal system

Miloš Velojić[1], Viktor Bertrandsson Erlandsson[2], Frank Melcher[2], Peter Onuk[2,3], Rade Jelenković[1] and Vladica Cvetković[1]

[1] Faculty of Mining and Geology, Djušina 5, Belgrade, Serbia; (milos.velojic@rgf.bg.ac.rs)
[2] Montanuniversität Leoben, Department Applied Geosciences and Geophysics, Peter-Tunner-Straße 5, Leoben, Austria
[3] Karl-Franzens University Graz, Institute of Earth Sciences, Austria

doi: 10.4154/gc.2022.25

Crossref Similarity Check

Article history:
Manuscript received October 25, 2021
Revised manuscript accepted May 19, 2022
Available online October 17, 2022

Abstract

Čukaru Peki is a recently discovered porphyry- high-sulfidation Cu-Au deposit located 5km south of the mining town of Bor in east Serbia. Three styles of mineralization are distinguished in the Čukaru Peki system: a high-sulfidation type with massive sulfides (named the Upper zone), a porphyry type (named the Lower zone) and a transition type (between porphyries and massive sulfides). This study investigates the concentration and distribution of trace elements in pyrite from these three mineralization zones of Čukaru Peki. The high-sulfidation pyrite contains elevated concentrations of V, Mn, Ni, Cu, As, Mo, Ag, Cd, In, Sn, Sb, Au, Hg, Tl, Pb and Bi, compared to pyrite from the porphyry zone. The porphyry zone pyrite contains elevated concentrations of Co and Se. The sample from the transition zone contains concentrations between the two other zones, with the exception of the relative enrichment of Co and Ag. This research also aims to separate different stages of ore deposition. The porphyry stage contains several types of veins: quartz A veins, quartz B veins, pyrite D veins, magnetite veins, purple anhydrite veins, sulfide veins and orange anhydrite veins. The high sulfidation stage also formed in several stages: pyrite1, pyrite-enargite veins, pyrite-covellite veins, pyrite2 veins and calcite-anhydrite veins. There are distinct differences between various vein generations found within each zone, notable examples are the enrichment of Se in quartz B veins pyrite and Cu in sulfide veins, compared to other veins from porphyry zone veins and the enrichment of several trace elements (Cu, Mo, Ag, Cd, In, Sn, Sb, Au, Hg, Tl, Pb and Bi) in pyrite from the Py-cov veins in comparison to the other high-sulfidation veins. The trace element data also indicates a change in fluid compositions; the earlier fluids responsible for the porphyry zone mineralization showing a slightly more magmatic fluid signature (higher Co/Sb and Se/As values) and the later high-sulfidation fluids bearing a more typical epithermal trace element signature, which indicates cooling and diluting of fluids. Some of the porphyry zone pyrite crystals (from B-type veins and Purple anhydrite-veins) contain elevated concentrations of elements attributed to the high-sulfidation zone (e.g. Cu, Ag, Cd, In, Sn, Pb and Bi), which suggests that these veins were affected by later high-sulfidation fluids.

Keywords: Porphyry copper, High-sulfidation Cu-As-Au, Pyrite, Trace elements, LA-ICP-MS, Timok magmatic complex, Bor metallogenic zone

1. INTRODUCTION

The Čukaru Peki hydrothermal system is part of the Bor metallogenic zone, which is hosted by the Timok magmatic complex (JANKOVIĆ, 1990; KOLB et al., 2013). This complex is considered to be the eastern segment of the large magmatic and metallogenic arc known as the Apuseni-Balkan-Timok-Srednogorje belt (ABTS belt, which is located in Romania, Serbia and Bulgaria (NEUBAUER, 2002). The ABTS belt is characterized by the presence of numerous porphyry and polymetallic ore deposits (Moldova Noua, Bor, Elatsite, Chelopech), which were formed during the subduction processes associated with the closure of the Neothetys Ocean, between 92 and 75 Ma (NEUBAUER, 2002; FÜGENSCHUH & SCHMID, 2005; GALLHOFER et al., 2015).

The magmatic activity in the Timok magmatic complex was manifested in two or three volcanic phases (DROVENIK, 1961; JANKOVIĆ, 1990), which altogether lasted around 10 Ma (VON QUADT et al., 2002). It is generally accepted that most of the significant ore deposits in this complex were formed during the first volcanic phase (JANKOVIĆ, 1990; KOLB et al.,2013; JELENKOVIĆ et al., 2016), which lasted from 89 to 84 Ma (VON QUADT et al., 2002). The simplified map of the Timok magmatic complex is shown in Fig.1.

The Bor metallogenic zone hosts several large porphyry deposits, which have been mined since the beginning of the 20th century (Bor, Majdanpek, Veliki Krivelj) as well as other genetic types of ore deposits, such as high-sulfidation epithermal (Tilva Mika, Kamenjar), low-sulfidation epithermal (Zlaće), hydrothermal-volcanogenic (Lipa, Kraku Bugaresku), skarns (Valja Saka) and recently discovered Carlin-type deposits (Korkan,Kraku Pešter and Bigar Hill) (JANKOVIĆ et al., 2002; JELENKOVIĆ et al., 2016). Estimated mineral resources of the entire zone are over 20 Mt of Cu and in excess of 1000 tonnes of Au (JELENKOVIĆ et al., 2016).

The Čukaru Peki hydrothermal system was located in 2011 and is one of the largest recently discovered Cu-Au deposits in south-eastern Europe. Preliminary estimations suggest that the total mineral resources of copper ore in this deposit could amount to between 500 and 1000 million tonnes grading more than 0,7 % Cu (JELENKOVIĆ et al.2016). It is located just 5km south of the mining town of Bor. BANJEŠEVIĆ & LARGE (2014) have

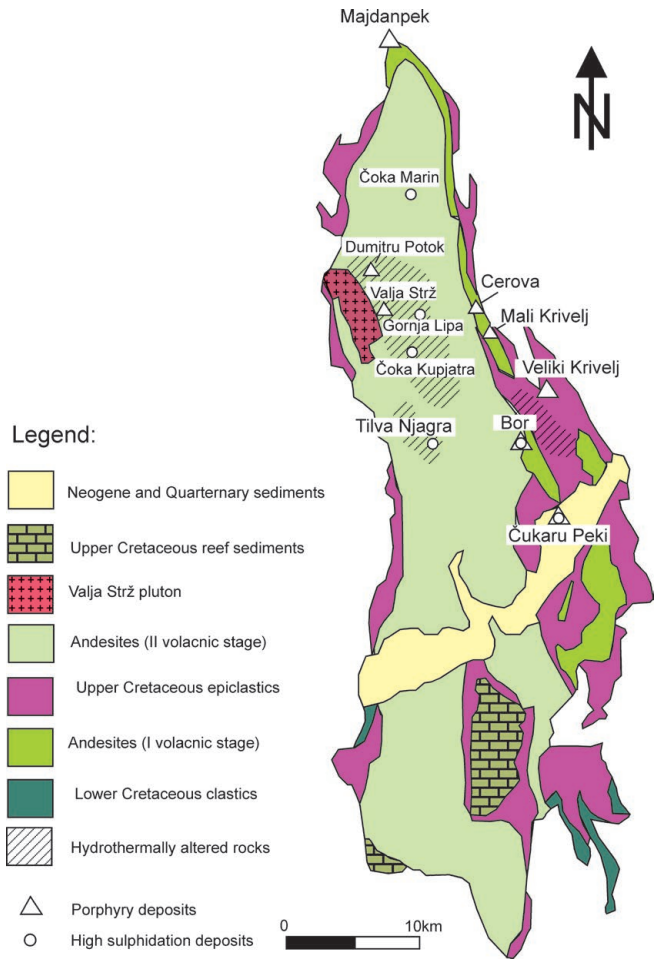

Figure 1. A simplified geological map of the Timok magmatic complex, adapted from PAČEVSKI et al. (2016) and JELENKOVIĆ et al. (2016).

genetically classified the Čukaru Peki system as a porphyry Cu-Au deposit with high-sulfidation epithermal (Cu-As-Au) massive sulfides.

Several authors have measured the concentrations and distribution of trace elements in the porphyry deposits in the Bor metallogenic zones and the results of these measurements were published in several reports and doctoral dissertations (PAVIĆEVIĆ et al. (1981, 1985), MIŠKOVIĆ (1989) and VAKANJAC (2000)). JANKOVIĆ et al. (2002) provide a synthesis of the obtained results of these studies and drew the following conclusions:

- Concentrations of Au are increased (up to 49 ppm) in several studied ore minerals, e.g. in chalcopyrite, pyrite and bornite.
- Above detection limit concentrations of Ag are present in almost all of the analyzed minerals.
- Enargite contains increased concentrations of Ge (up to 0,46%).
- Palladium concentrations are increased (up to 0,5%) in different ore minerals: pyrite, chalcopyrite, bornite, digenite, covellite, luzonite and tetrahedrite, probably in the form of mineral inclusions.
- Selenium concentrations are increased (up to 0,5%) in bornite and covellite.
- In most sulfide minerals, there is a notable enrichment (from 0,2 to 0,6%) of trace elements, such as Sn, Te, W, Se etc.

In this study we report and discuss new results from LA-ICP-MS analyses of trace elements (S, V, Cr, Mn, Fe, Co, Ni, Cu, As, Se, Mo, Ag, Cd, In, Sn, Sb, Au, Hg, Tl, Pb and Bi) in pyrite grains from different zones and veins of the Čukaru Peki deposit, with a special emphasis on the distribution of trace elements in pyrite from different mineralization zones and ore veins. This research will contribute to a better identification of the veins and minerals in Čukaru Peki that concentrate rare and precious elements, such as gold and silver. The identification will be particularly significant for the extraction of gold from the high-sulfidation zone.

2. GEOLOGICAL SETTING

The hydrothermal system of Čukaru Peki is hosted by intermediate volcanic and plutonic rocks formed during the first volcanic phase of the Timok magmatic complex (JELENKOVIĆ et al., 2016 and references therein). The volcanic rocks are represented by two distinct types of andesites: altered plagioclase-hornblende phyric, holocrystalline andesites (also called Lower andesites) and unaltered hornblende-plagioclase phyric, hypocrystalline andesites (known as Upper andesites) (JAKUBEC et al., 2018). The volcanics are overlain by Upper Cretaceous sediments, which consist of three sedimentological units: 1) the Oštrelj formation with grey siltstone and marl (uppermost) 2) the Metovnica formation with red marl and epiclastics and 3) the lowermost coarse-grained Bor clastites (BANJEŠEVIĆ et al., 2019) (Fig. 2).

Post-Cretaceous deformation created a series of eastward-dipping faults and caused the formation of basins which were filled with Miocene sediments. The most prominent structure in this region is the Bor Fault that splits into 2 structures, called the Bor 1 and Bor 2 faults, which are considered to be the eastern boundaries of the mineralized zone at Čukaru Peki. These structures also cut through the Miocene sedimentary fill (JAKUBEC et al., 2018). The process of basin formation was important for the preservation of Cretaceous ore deposits in the Timok Magmatic Complex from subsequent erosion (KNAAK et al., 2016). The Miocene sediments in this area have a thickness of 200-400 m and have a discordant boundary with the Cretaceous sediments (Fig. 3) (JAKUBEC et al., 2018).

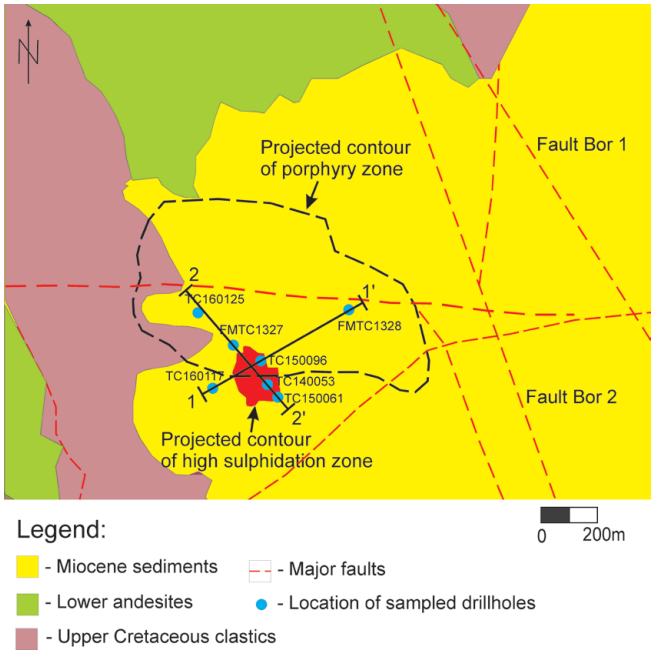

Figure 2. A simplified geological map of the area around the Čukaru Peki ore deposit, with the location of major faults, sections and sampled drillholes.

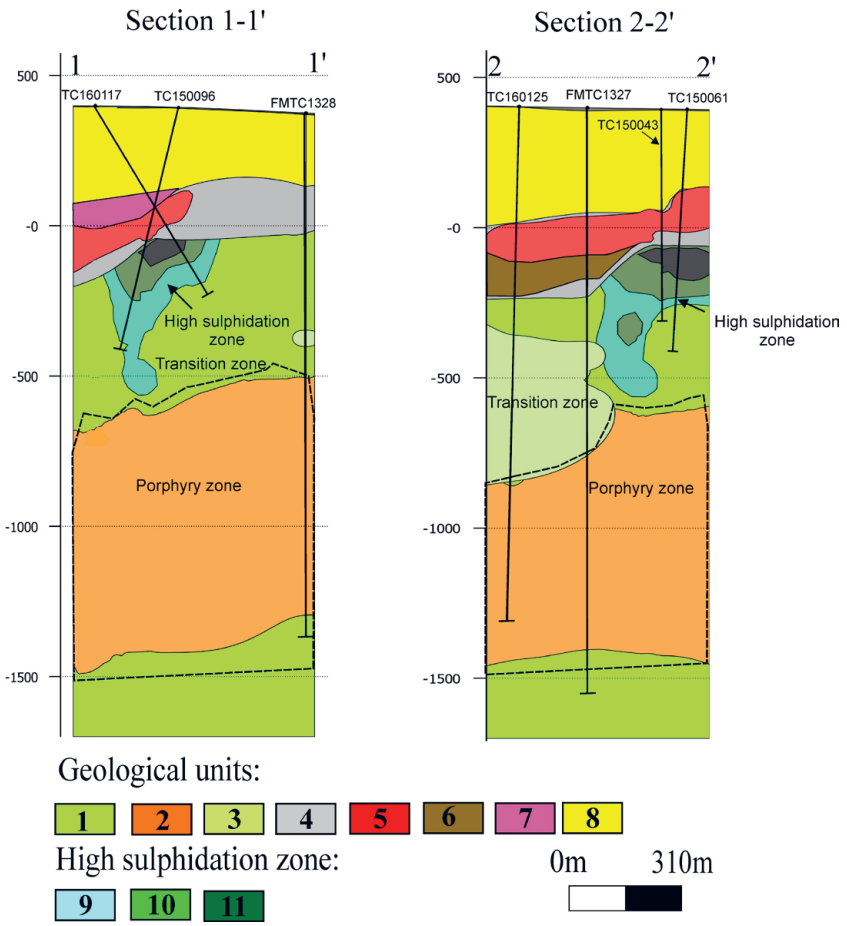

Figure 3. Simplified cross-sections through the Čukaru Peki ore deposit, modeled using Leapfrog software, showing zones with different types of mineralization. Legend: 1- Lower andesites; 2- Diorite porphyries; 3- Brecciated zone; 4-Upper andesites; 5- Upper Cretaceous marl; 6- Cretaceous epiclastics; 7- Upper Cretaceous clastics (Bor conglomerates); 8- Cenozoic sediments; 9- Massive sulfides with more than 0,5% Cu; 10- Massive sulfides with more than 1% Cu; 11- Massive sulfides with more than 2% Cu.

JELENKOVIĆ et al. (2016) have distinguished three zones of mineralization in the Čukaru Peki hydrothermal system:

1) A high-sulfidation zone consists of massive sulfides, pyrite-covellite veins and hydrothermal breccias. This type of mineralization forms a localized zone, with a horizontal area of 300x300m and a vertical extent of 500 - 600 m and it is located at depths between 400 and 1000m from the surface., which contains the highest grades of Cu (5-19%) and Au (3-12g/t) (JAKUBEC et al., 2018). With increasing depth, the mineralization contains less pyrite and becomes more characterized by veins and stockworks. The dominant type of alteration is advanced argillic alteration, with abundant residual vuggy silica, alunite and subordinate dickite (JAKUBEC et al., 2018). The boundary of this zone is represented by a clay-rich argillic alteration (kaolinite+pyrite) halo around massive sulfides. The main Cu-bearing minerals in the high- sulfidation zone (Upper zone) are covellite and enargite, whereas the dominant Cu-bearing mineral in the porphyry zone (Lower zone) is chalcopyrite, with subordinate bornite. Preliminary ore microscopic examinations imply that Au is present in two forms in the high-sulfidation zone of Čukaru Peki: 1) as tellurides such as calaverite (AuTe2), sylvanite (Au,Ag)2Te4 and kostovite (AuCuTe4); and 2) Sub-microscopic native Au, hosted in pyrite or sometimes bornite (JAKUBEC et al., 2018).

2) The transition epithermal zone is located between the high-sulfidation zone and the porphyry zone. It is characterized by the replacement of early sulfides (chalcopyrite) with high-sulfidation minerals (covellite and enargite). 2) Anhydrite, calcite and gypsum are the three main types of vein in this zone. The main type of alteration is argillic alteration (smectite- + montmorillonite) (JAKUBEC et al., 2018), which sporadically overprints the porphyry-type alterations.

3) The porphyry zone is mostly hosted by diorites and overlying andesites. The dimensions and shape of the porphyry zone have not yet been determined, due to its great depth; it is located at between 750m to more than 2200m from the surface. The dominant types of alteration are potassic alteration and chloritization. Quartz veins (with chalcopyrite, pyrite and bornite), magnetite veins (with magnetite, hematite and chalcopyrite) and anhydrite veins (with pyrite and subordinate chalcopyrite and bornite) are the main types of veins (VELOJIĆ et al., 2020).

3. SAMPLES AND METHODS

Reflected light microscopy and SEM measurements were performed on samples from the Upper, Transition and Lower zones of Čukaru Peki. Analyses were performed at Montanuniversität Leoben, Austria and University of Belgrade- Faculty of Mining and Geology, Serbia.

3.1. Laser ablation inductively coupled plasma mass spectrometry (LA-ICP-MS)

Trace element analyses were conducted on 5 samples from the Upper zone (cp012, cp018, cp028, cp038A, and cp073), one from

Geologia Croatica

Table 1. Location and description of samples used for the measurements of trace elements by LA-ICP-MS. Abbreviations: py-pyrite; cov-covellite; en-enargite; su-sulfide.

Sample ID	Drillhole	Ore zone	Vein description
CP012	TC150096	High-sulfidation	Pyrite-covellite (py-cov) vein with clasts of Py1 pyrite.
CP018	TC150096	High-sulfidation	Pyrite-enargite (py-en) vein.
CP028	TC150061	High-sulfidation	Pyrite-covellite (py-cov) vein.
CP038A	TC160117	High-sulfidation	Pyrite-covellite (py-cov) vein.
CP073	TC150043	High-sulfidation	Pyrite-enargite (py-en) vein.
CP084	FMTC1327	Porphyry	Quartz B vein.
CP115	FMTC1328	Porphyry	Sulfide vein (Su type).
CP117	FMTC1328	Porphyry	Sulfide vein (Su type).
CP119	FMTC1328	Porphyry	Purple anhydrite vein.
CP122	FMTC1328	Porphyry	Pyrite vein (type D).
CP126	TC160125	Transition	Py1 pyrite.

the transition zone (cp126) and 5 samples from the Lower zone of Čukaru Peki (cp084, cp115, cp117, cp119 and cp122). A description and location of all samples is shown in table 1 and the locations of drillholes are shown on Figs 2 and 3.

Pyrite analyses were carried out using a Nd:YAG laser ablation system coupled to an Agilent 8800 ICP-MS at the Department of Applied Geosciences and Geophysics, Montanuniversität Leoben in Austria. Pyrite crystals were ablated with a spot size of 50 µm and an on-mineral laser fluency of 2-3 J/cm^2, at a 10 Hz repetition rate. Helium was used as the carrier gas with a flow rate of 0.75 L/min, which was mixed with Ar during transport to the ICP-MS. Isotopes measured were: ^{34}S, ^{51}V, ^{52}Cr, ^{55}Mn, ^{57}Fe, ^{59}Co, ^{60}Ni, ^{63}Cu, ^{75}As, ^{82}Se, ^{95}Mo, ^{107}Ag, ^{111}Cd, ^{115}In, ^{118}Sn, ^{121}Sb, ^{197}Au, ^{201}Hg, ^{205}Tl, ^{208}Pb and ^{209}Bi. The spot analysis procedure includes a 30 sec pre-ablation background collection, followed by 60 sec of laser ablation and data acquisition. Individual ablation cycles were followed by a 30 sec washout delay. Quantification of the element concentrations of pyrite were calculated using ^{34}S as the internal standard. Data reduction was performed with the Iolite 4 software (PATON et al., 2011). The in-house sphalerite matrix-matched sinter pressed powder pellet reference material MUL-ZnS1 (ONUK et al., 2017) was used as the primary external standard. The MASS-1 USGS powder pressed polysulfide certified reference material (WILSON et al., 2002) was used as the external standard for the quantification of Au, Tl and Hg, as the reference material MUL-ZnS-1 is not suitable for quantification of these elements. The MASS-1 was also used for quality control of the analyses. Both reference materials were analyzed every 20 spots for the correction of instrumental drift. Detection limits were calculated by the 'Howell et al. 2010' method option within the Iolite 4 software (Table 2).

Table 2. Calculated median detection limits of each element measured by LA-ICP-MS.

Detection limits (µg/g).			
V	0.034	Cd	0.98
Cr	0.34	In	0.018
Mn	0.18	Sn	0.15
Co	0.056	Sb	0.054
Ni	0.20	Au	8E-07
Cu	1.2	Hg	0.28
As	2.6	Tl	0.0037
Se	4.1	Pb	0.024
Mo	0.047	Bi	0.0053
Ag	0.0081		

Laser ablation spots were set out carefully to avoid inclusions, cracks or other visible impurities that could interfere with the measured data. Due to pyrite crystals most commonly being zoned, it was challenging to acquire time-count signals for a single zone. Thus, it is also difficult to discriminate exotic inclusions from chemical zoning in pyrite as several elements in a Cu-Au system could be attributed to pyrite zoning or separate phases. This may result in a wider range of trace element concentrations in a mineral population, as data was included rather than deleted when uncertain of zoning vs. inclusion. Due to the generally low concentrations of many trace elements in Čukaru Peki (many being below detection limits), values that are below the detection limits are replaced with half the respective detection limit in the production of plots and diagrams in this study. This is a commonly used approach for handling such data.

4. RESULTS

4.1. Petrography

Macroscopic observations of veins and their crosscutting relationhips, as well as reflected light microscopy of polished sections imply that the chronological order of deposition of mineralizing stages in the high-sulfidation (Upper) zone of Čukaru Peki is as follows: 1) Fine-grained pyrite (Py1) 2) Pyrite-enargite (Py-en) veins 3) Pyrite-covellite (Py-cov) veins 4) Py2 veins and 5) Marcasite veins. A paragenetic sequence of the main ore stages is shown in table 3 and the main characteristics of individual stages are discussed below:

1) Fine-grained pyrite (Py1): Replacement of rocks by very fine-grained pyrite is omnipresent in the Upper zone of Čukaru Peki. It was probably preceded by advanced argillic alteration of rocks (with quartz and alunite) (Figs.4a and 4c). This pyrite also contains subordinate rutile, but no other sulfide minerals (Fig. 5a). This pyrite phase is also present within the transition zone.

2) Pyrite-enargite (Py-en) veins: This type of vein is common in the deeper parts of the Upper zone (Figs.4a and 4b). They contain intergrown grains of enargite and pyrite, with subordinate luzonite (Fig.5b). The main gangue mineral in these veins is cryptocrystalline quartz (similar to chalcedony). It is commonly observed that these veins are crosscut by subsequent thin veins with pyrite and covellite (Fig.4b).

3) Pyrite-covellite (Py-cov) veins: This is the most common type of vein in the shallow parts of the Upper zone (Fig.4b and 4c). The veins mostly contain covellite, pyrite and enargite, but sometimes also occur as monomineralic covellite veins (Fig.5b and 5c). Pyrite in these veins often exhibits colloform textures. Zonation can occasionally be recognized in these veins, with colloform pyrite and enargite filling the outer parts of veins and covellite with gypsum filling the middle part.

4) Pyrite2 (Py2) veins: This is a rare type of thin grey veinlets that crosscut py-cov veins. They are quartz veins which contain very small euhedral pyrite grains. (Fig.5d).

5) Marcasite veins: These veins contain large grains of colloform marcasite, with subordinate arsenopyrite and small grains of colloform sphalerite (Fig.5e).

The transitional epithermal zone contains the same types of veins like the paragenetically later parts of the porphyry zone (purple anhydrite veins, sulfide veins and orange anhydrite veins), as well as Py1 pyrite, which is also found in the high-sul-

Table 3. Paragenetic sequence of mineralization in the high-sulfidation (Upper) zone of Čukaru Peki.

	Py1 pyrite	Py-en veins	Py-cov veins	Py2 veins	Marcasite veins
Pyrite					
Quartz					
Enargite					
Covellite					
Gypsum					
Luzonite					
Colusite					
Rutile					
Marcasite					
Arsenopyrite					
Sphalerite					

Abbreviations: Py- pyrite; Cov- covellite; En- enargite

fidation zone. The main ore minerals in this zone are covellite, chalcopyrite, digenite and enargite with occasional native sulfur. The dominant type of alteration is argillic alteration (with quartz, clay minerals and sericite).

In the porphyry (Lower) zone of Čukaru Peki, several types of veins can be distinguished. Most of these veins fit into the general model of veins in porphyry systems (e.g. Sillitoe, 2010), so the names from the general model are used for the description of these veins. The sequence of main ore veins is shown in Table 4 and the main characteristics of veins are shown below (VELOJIĆ et al 2020):

1) Quartz veins (type A): Wiggly high temperature quartz veins that do not contain ore minerals.

2) Quartz veins (type B): Mostly occur as stockwork veins which contain chalcopyrite, with subordinate pyrite and bornite (Fig.4d, Fig. 5f). They are usually accompanied by phyllic alteration (with potassic feldspar and secondary biotite, with subordinate magnetite and anhydrite). Small grains of native gold and electrum were also detected in these veins by SEM examination (Fig. 6b and 6d).

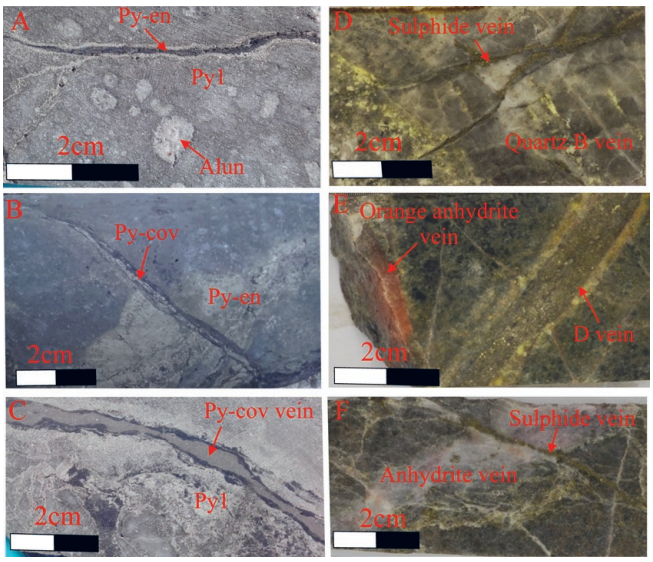

Figure 4. Crosscutting relationhips of different veins in the Čukaru Peki system. A) Py-en vein in andesite altered by advanced argillic alteration (with grains of alunite) and Py1 pyrite, TC150096 564m; B) Py-cov vein crosscutting py-en vein, TC150062 592m; C) Py-cov vein crosscutting Py1 pyrite, TC150096 564m; D) Sulfide vein crosscutting a quartz B vein, FTMC1328 1348,5m; E) D vein, crosscut by a thin orange anhydrite vein FMTC1328 1581.5m; F) Thin sulfide vein crosscutting a purple anhydrite vein FMTC1327 1589.2m

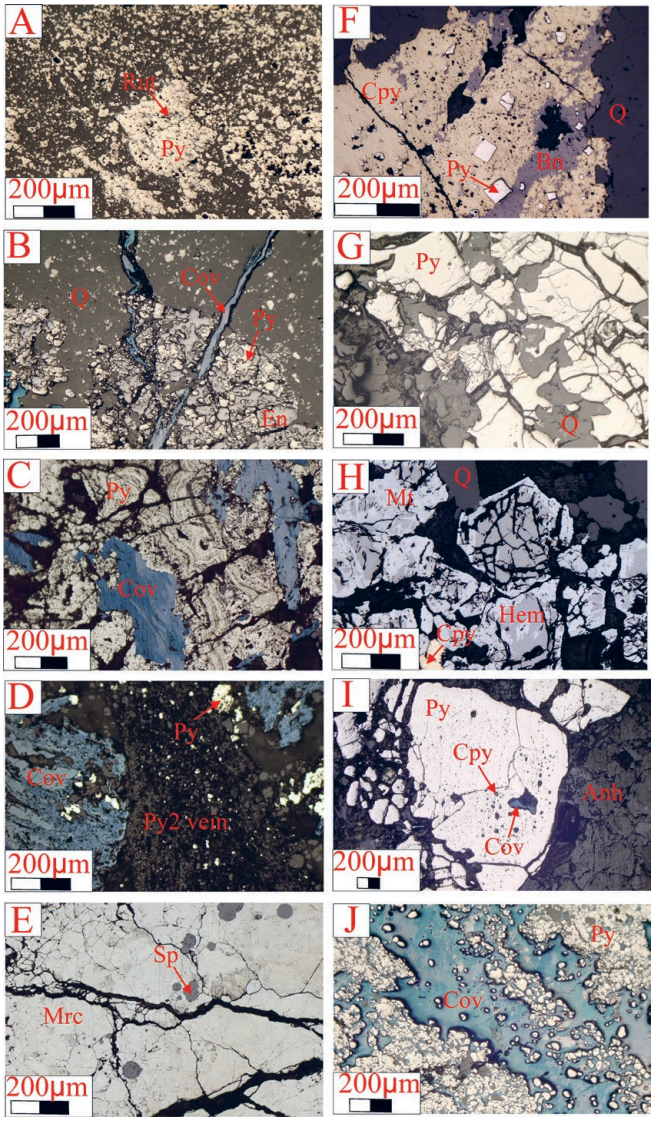

Figure 5. Reflected light photomicrographs of samples of different types of ore veins in Čukaru Peki. A) Py1 pyrite with small grains of rutile, TC150096 476.8 m; B) Thin covellite vein crosscutting a wide py-en vein with enargite and pyrite, TC150043 591.4 m; C) Py-cov vein with covellite and colloform pyrite, TC160117 535 m; D) Py2 vein with small pyrite grains crosscutting a covellite vein, TC150096 448m; E) Colloform marcasite vein with small grains of round colloform sphalerite, TC150061 505.5 m; F) Quartz B vein with chalcopyrite, bornite and pyrite, FMTC1327 1246.5 m; G) Pyrite vein type; D, FMTC1328 1581.5 m; H) Magnetite vein with magnetite, partially replaced by hematite and small chalcopyrite grains, TC160125, 1644m; I) Anhydrite vein with a large pyrite grain with inclusions of covellite, FMTC1328 1442 m; J) Sulfide vein with covellite and pyrite, FMTC1328 1312.8 m.

3) Pyrite veins (type D): These veins contain relatively large and connected pyrite grains, which contain small inclusions of chalcopyrite, bornite and rutile (Fig. 5g). These veins are usually accompanied by chlorite alteration (with chlorite, haematite and sericite) (Fig.4e).

4) Magnetite veins (type M): Common veins in the deeper parts of the porphyry zone. They contain magnetite and hematite, with subordinate pyrite and chalcopyrite (Fig.5h). Magnetite is commonly replaced by hematite in a martitization process.

5) Purple anhydrite veins: These veins have a distinct purple-pink colour and are usually several centimetres wide. The most abundant mineral is pyrite, with smaller grains of chalcopyrite, covellite, chalcocite and bornite (Fig. 5i, Fig. 6c). They are common in both the porphyry and transition epithermal zones.

6) Sulfide (Su) veins : These veins are characterized by the presence of pyrite and covellite, with accompanying anhydrite (Fig. 5j). Like the previous type, these veins are also common in the transition epithermal zone. It is commonly observed that these veins crosscut earlier quartz and anhydrite veins (Fig.4d and 4f).

7) Orange anhydrite veins: They can be distinguished from purple anhydrite veins by colour, the shape of the anhydrite crystals and the absence of any ore minerals. These veins are clearly late, since they crosscut all the aforementioned veins (Fig.4e).

4.2. Pyrite trace element variations between the ore zones and intra-zonal variations

Median values of measurements on pyrite from the three ore zones (high-sulfidation, transition zone and porphyry zone) indicate a general trend of trace elements being enriched in the high-sulfidation zone, compared to the porphyry zone. High-sulfidation zone pyrite is enriched in V, Mn, Ni, Cu, As, Mo, Ag, Cd, In, Sn, Sb, Au, Hg, Tl, Pb and Bi, relative to porphyry zone pyrite (as seen in table 5.) One sample of pyrite from the transition zone was analyzed and it contains concentrations that fall in-between the two other zones, most commonly showing values similar to the porphyry zone. Cobalt, As and Ag are the only outliers of this trend. Cobalt is significantly enriched in the sample from the transition zone (median 64 µg/g) compared to pyrite from both other zones (porphyry with 16 & high-sulfidation with 1.7 median µg/g). Arsenic is depleted in transition zone pyrite (median 2.3 µg/g), whereas porphyry zone pyrite has slightly higher concentrations with a median value of 16 µg/g. Silver shows similar concentrations in both the Ag-rich sample from the transition zone and high-sulfidation zone (median 10 µg/g). Nickel is also rather anomalous as it shows values more similar to the high-sulfidation zone pyrite, although the median concentrations are just between 2.3 and 6.7 µg/g.

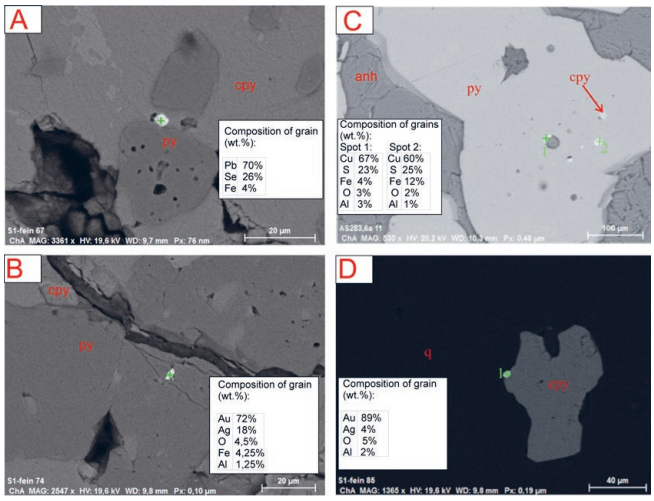

Figure 6. BSE image s taken during SEM analysis of samples from Čukaru Peki. A) Clausthalite (lead selenide) grain in a Quartz vein type B, FMTC1327 1246.5 m; B) Grain of electrum in a Quartz vein type B, FMTC1327 1246.5 m; C) Grain of pyrite from a purple anhydrite vein containing inclusions of chalcopyrite, chalcocite (spot 1) and bornite (spot 2), FMTC1328, 1442m; D) Chalcopyrite grain containing a small inclusion of native Au FMTC1327 1246.5 m. Chalcopyrite grain containing a small inclusion of native Au FMTC1327 1246.5 m.

Porphyry zone pyrite is significantly enriched in Co (median 16 µg/g) and Se (median 39 µg/g). Except for three spot measurements, porphyry zone pyrite shows concentrations of both In and Sn as being below the detection limit.

Although there are characteristic trace element trends between the zones, it is important to note that these trends are not always true for each vein type within each ore zone (Fig.7). For example, Se that is generally enriched in the porphyry zone, shows significantly lower concentrations in pyrite from the anhydrite veins of the porphyry zone.

All measurements of porphyry zone pyrite show values below the detection limits for In and Sn, except for three spots from the B-type veins. These three spots also show elevated concentrations of other elements characteristic of the high-sulfidation zone, i.e. Mn, Cu, Ag, Cd, Pb and Bi. This is also the case for Cd in anhydrite-veins, where only two spot measurements show elevated Cd contents. Due to these elevated contents of elements typically found in high-sulfidation veins, B-type pyrite crystals show a wide spread in concentrations for the analyzed elements. D-type pyrite shows significantly lower median concentrations for several metals (Cu, Ag, Au and Bi), compared to the other porphyry pyrite crystals. All these elements are typically low in pyrite from the porphyry zone. Anhydrite-vein pyrite shows trace element concentrations typical for the general porphyry

Table 4. Paragenetic sequence of veins in the porphyry (Lower) zone of Čukaru Peki (Modified after VELOJIĆ et al., 2020).

	Quartz B veins	Pyrite D veins	Magnetite veins	Purple anhydrite veins	Sulfide veins
Pyrite	—	—	—	—	—
Chalcopyrite	—			—	
Bornite	—			—	
Magnetite			—		
Hematite			—		
Pyrrhotite			—		
Rutile	—	—	—	—	—
Covellite				—	—
Enargite				—	—

Table 5. Statistical summary for LA-ICP-MS pyrite data from the three different Čukaru Peki ore zones. All values are in µg/g. N: total number of measurements; n: number of measurements below detection limit out of N. N may vary within a pyrite population between elements due to obvious inclusions, which have been removed from the dataset. When there are more measurements below the detection limits than above (n > N), median values are indicated by "<detection limit value". When N > n, n is replaced with ½ the median detection limit value of the element, for median calculations. DL: median detection limit value of all measurements for each element.

	Porphyry zone									
	Quartz veins (type B)					**Pyrite veins (type D)**				
	N	n	Median	Min	Max	N	n	Median	Min	Max
V	6	4	<0.034	<0.034	0.24	15	15	<0.034	<0.034	<0.034
Cr	6	6	<0.34	<0.34	<0.34	15	15	<0.34	<0.34	<0.34
Mn	5	0	11	11	19	15	0	11	10	11
Co	6	0	13	0.10	961	15	0	35	0.33	232
Ni	6	2	2.3	<0.2	198	15	1	3.1	0.43	11
Cu	6	1	813	<1.2	6098	15	0	8.2	1.1	81
As	6	4	<2.6	<2.6	27	15	15	<2.6	<2.6	<2.6
Se	6	0	717	437	1041	15	0	64	28	113
Mo	6	6	<0.047	<0.047	<0.047	15	15	<0.047	<0.047	<0.047
Ag	6	1	0.81	<0.0081	1.1	15	10	<0.0081	<0.0081	0.023
Cd	6	3	0.70	<0.98	3.2	15	15	<0.98	<0.98	<0.98
In	6	3	0.35	<0.018	2.3	15	15	<0.018	<0.018	<0.018
Sn	5	2	1.00	<0.15	24	15	15	<0.15	<0.15	<0.15
Sb	6	6	<0.054	<0.054	<0.054	15	15	<0.054	<0.054	<0.054
Au	6	1	0.016	<8E-07	0.46	15	12	<8E-07	<8E-07	0.0011
Hg	6	6	<0.28	<0.28	<0.28	15	14	<0.28	<0.28	0.34
Tl	6	3	0.0046	<0.0037	0.022	15	13	<0.0037	<0.0037	0.021
Pb	6	1	96	<0.024	278	15	15	<0.024	<0.024	<0.024
Bi	5	1	0.26	<0.0053	8.8	15	15	<0.0053	<0.0053	<0.0053

	Porphyry zone									
	Purple anhydrite vein					**Sulfide (Su) vein**				
	N	n	Median	Min	Max	N	n	Median	Min	Max
V	15	15	<0.034	<0.034	<0.034	25	20	<0.034	<0.034	0.087
Cr	15	14	<0.34	<0.34	0.98	29	23	<0.34	<0.34	3.6
Mn	12	0	11	10	18	29	0	12	11	16
Co	15	1	104	<0.056	158	23	0	3.6	0.072	65
Ni	15	3	2.0	<0.2	7.3	24	3	0.45	<0.2	6.6
Cu	10	0	43	2.9	132	21	0	1561	17	4163
As	15	15	<2.6	<2.6	<2.6	28	28	<2.6	<2.6	<2.6
Se	13	0	40	27	108	25	16	<4.1	<4.1	79
Mo	15	15	<0.047	<0.047	<0.047	26	26	<0.047	<0.047	<0.047
Ag	15	7	0.0041	<0.0081	0.14	29	6	0.12	<0.0081	2.9
Cd	15	13	<0.98	<0.98	1.6	29	29	<0.98	<0.98	<0.98
In	15	15	<0.018	<0.018	<0.018	27	27	<0.018	<0.018	<0.018
Sn	15	15	<0.15	<0.15	<0.15	27	27	<0.15	<0.15	<0.15
Sb	15	15	<0.054	<0.054	<0.054	28	24	<0.054	<0.054	0.16
Au	15	0	0.0031	E2.3-05	0.029	29	8	0.082	<8E-07	1.0
Hg	15	15	<0.28	<0.28	<0.28	29	8	0.33	<0.28	0.93
Tl	15	11	<0.0037	<0.0037	0.029	29	15	<0.0037	<0.0037	0.11
Pb	12	7	<0.024	<0.024	1.4	26	7	0.25	<0.024	14
Bi	12	7	<0.0053	<0.0053	0.39	29	5	0.048	<0.0053	2.3

Table 5. Continued

	Transition					High-Sulfidation				
	Fine-grained pyrite (Py1)					**Fine-grained pyrite (Py1)**				
	N	n	Median	Min	Max	N	n	Median	Min	Max
V	6	1	0.13	<0.034	0.33	5	0	4.9	1.1	5.7
Cr	8	2	0.57	<0.34	1.3	8	1	1.5	0.17	3.3
Mn	8	0	9.6	8.9	11	7	0	59	16	81
Co	8	0	64	24	88	9	0	66	11	91
Ni	8	0	5.0	2.8	11	9	0	15	7.9	17
Cu	8	0	6442	4324	7787	9	0	9654	7881	16211
As	7	0	2.3	1.9	3.0	9	0	88	26	218
Se	8	0	20	8.7	123	9	1	14	<4.1	17
Mo	8	8	<0.047	<0.047	<0.047	8	0	0.42	0.15	1.1
Ag	8	0	10	7.4	21	9	0	5.7	2.5	11
Cd	8	8	<0.98	<0.98	<0.98	9	9	<0.98	<0.98	<0.98
In	8	8	<0.018	<0.018	<0.018	9	1	0.11	<0.018	0.37
Sn	8	1	0.35	<0.15	0.71	9	0	2.8	1.4	8.6
Sb	8	0	0.21	0.11	0.38	9	0	1.7	0.75	3.3
Au	8	0	0.85	0.64	2.4	9	0	4.0	2.0	20
Hg	8	0	0.52	0.26	0.89	9	3	0.57	<0.28	1.3
Tl	8	0	0.81	0.45	2.9	9	0	24	0.60	140
Pb	8	0	25	10	81	9	0	92	44	797
Bi	8	0	0.97	0.54	1.5	9	0	9.5	1.7	45

	High-Sulfidation									
	Pyrite-enargite (Py-en) veins					**Pyrite-covellite (Py-cov) veins**				
	N	n	Median	Min	Max	N	n	Median	Min	Max
V	14	0	0.17	0.030	3.3	18	0	6.3	0.68	43
Cr	20	14	<0.34	<0.34	1.7	28	4	1.5	<0.34	22
Mn	18	0	11	8.8	125	26	0	23	9.6	606
Co	20	2	5.3	<0.056	101	29	2	0.19	<0.056	12
Ni	20	1	2.3	<0.2	25	28	0	6.4	0.77	30
Cu	18	0	11066	151	32781	27	0	16545	10453	35235
As	17	10	<2.6	<2.6	23	27	0	66	24	222
Se	20	1	12	<4.1	47	26	2	7.7	<4.1	69
Mo	19	12	<0.047	<0.047	1.1	24	0	1.3	0.13	33
Ag	20	0	1.2	0.061	14	29	0	34	7.1	186
Cd	20	20	<0.98	<0.98	<0.98	29	9	5.9	<0.98	31
In	20	16	<0.018	<0.018	0.14	27	0	2.0	0.18	12
Sn	20	12	<0.15	<0.15	6.6	29	0	11	0.68	33
Sb	20	4	0.20	<0.054	1.6	29	0	5.9	1.0	18
Au	20	0	0.60	0.021	14	29	0	20	2.7	55
Hg	20	13	<0.28	<0.28	1.5	29	2	6.3	<0.28	28
Tl	20	2	0.018	<0.0037	16	29	0	56	6.9	657
Pb	16	0	1.5	0.30	254	28	0	1224	317	4967
Bi	19	0	0.65	0.052	5.1	29	0	27	6.8	103

zone trends. Two out of the fifteen analyzed spots show elevated Cd values, as mentioned previously, which is a major deviation from the porphyry zone trend.

Together with D-type pyrite, the anhydrite-vein pyrite has the lowest median Cu concentrations among the porphyry zone pyrite crystals (8.2 and 43 μg/g respectively). Median Co concen-

trations are the highest in the anhydrite-vein pyrite crystals with 104 µg/g. Sulfide-vein pyrite crystals have the lowest median Co and Ni concentrations (3.6 and 0.45 µg/g respectively) of all the porphyry zone pyrite crystals. The Co concentrations are in fact more similar to that of pyrite-enargite vein pyrite (median 5.3 µg/g) in the high-sulfidation zone, although this pyrite has a higher median Ni concentrations (2.3 µg/g). Selenium is generally enriched in the porphyry zone pyrite, but sulfide-vein pyrite contains the lowest median Se concentrations (<4.1 µg/g) out of all the pyrite populations measured, with 16 out of 25 measurements showing values for Se that are below detection limits.

Pyrite1 is the only pyrite type specifically found in two zones, the transition and high-sulfidation zones. This is evident in the trace element concentrations, as they have relatively similar median values in several of the measured elements (Co, Cu, Se, Cd and Hg). Accordingly, pyrite1 from the high-sulfidation zone is significantly enriched in a range of elements: V, Cr, Mn, Ni, As, Sn, Sb, Au, Tl, Pb and Bi. Thus, the high-sulfidation Pyrite1 and pyrite from the pyrite-enargite vein shows the typical high-sulfidation trace element enrichment trend (eg. SYKORA et al.,2018), compared to the trend of the transition zone. Silver, Au, Pb and Bi in pyrite1 crystals show the lowest concentrations of all the high-sulfidation zone pyrite (median 1.2, 0.60, 1.5 and 0.65 µg/g respectively). These concentrations are still slightly, to significantly, higher than the porphyry zone pyrite median values.

The high-sulfidation pyrite-covellite veins are the most trace element-rich veins (e.g. Cu, Ag, Au and Pb) of the Čukaru Peki ore system and are considered to be paragenetically the last veins formed, of those veins analyzed in this study (as demonstrated in Figs.4B and 4C). Pyrite-covellite veins are significantly enriched in Cu, Mo, Ag, Cd, In, Sn, Sb, Au, Hg, Tl, Pb and Bi, even in comparison to the other high-sulfidation zone pyrite that are also commonly enriched in these elements. Pyrite-covellite veins are the only vein type with substantial Cd concentrations (median 5.9 µg/g), only 9 out of 29 measurements showing values below detection limits. The only other Cd measurements above detection limit are 5 (out of 65) spot measurements from the porphyry zone.

5. DISCUSSION

5.1. Stages of mineralization

There are distinct mineralogical differences between the three zones of mineralization in the Čukaru Peki hydrothermal system. The Upper zone consists of massive sulfides with pyrite-enargite and pyrite-covellite veins. The transitional epithermal zone consists of a system of anhydrite and gypsum veins, whereas the main ore minerals in this zone are covellite, chalcopyrite, digenite and enargite with occasional native sulfur. Mineralization in the Lower zone is mostly hosted by quartz and anhydrite veins with chalcopyrite, pyrite, bornite, magnetite, and pyrrhotite as the main ore minerals.

Ore microscopic examinations of samples from the Upper zone mineralization (high-sulfidation zone) of Čukaru Peki imply that this zone was formed in several successive stages: 1) Massive pyrite (Py1); 2) Py-en veins with pyrite and enargite; 3) Py-cov veins with pyrite, covellite and enargite; 4) Py2 veins with fine-grained pyrite and 5) Marcasite veins with arsenopyrite and sphalerite.

The research conducted by VELOJIĆ et al. (2020) implies that the Lower zone mineralization at Čukaru Peki formed in two successive stages. The porphyry stage formed at temperatures between 600 and 400°C and consists of four types of veins: 1) quartz veins type A without mineralization; 2) quartz veins type B with chalcopyrite, pyrite and bornite; 3) pyrite veins type D with subordinate chalcopyrite and bornite and 4) magnetite veins with hematite, pyrrhotite and chalcopyrite. The younger epithermal stage formed at temperatures between 300 and 200°C and includes three types of veins: 1) purple anhydrite veins with pyrite, with subordinate chalcopyrite, covellite and enargite; 2) sulfide veins with pyrite and covellite and 3) orange anhydrite veins without mineralization.

5.2. Zonal differences and trends in pyrite trace element composition

Several distinctions can be made between pyrite from the different mineralization zones of Čukaru Peki (Fig.8). Selenium and Co concentrations are relatively high in the porphyry zone (maximum median value of Co at 104 µg/g and Se at 717 µg/g) and gradually decrease (minimum median value of Co at 0.19 µg/g and Se at 7.7 µg/g; Fig.8a), whereas the opposite is observed for Au, Ag, As and Cu, which are significantly enriched in pyrite from the high-sulfidation zone (Fig.8c, 8d). Notable trends are observed with Ni and Co concentrations (Fig.8b), which are increased in purple anhydrite-veins and in transition zone pyrite, but are depleted in porphyry and high-sulfidation veins.

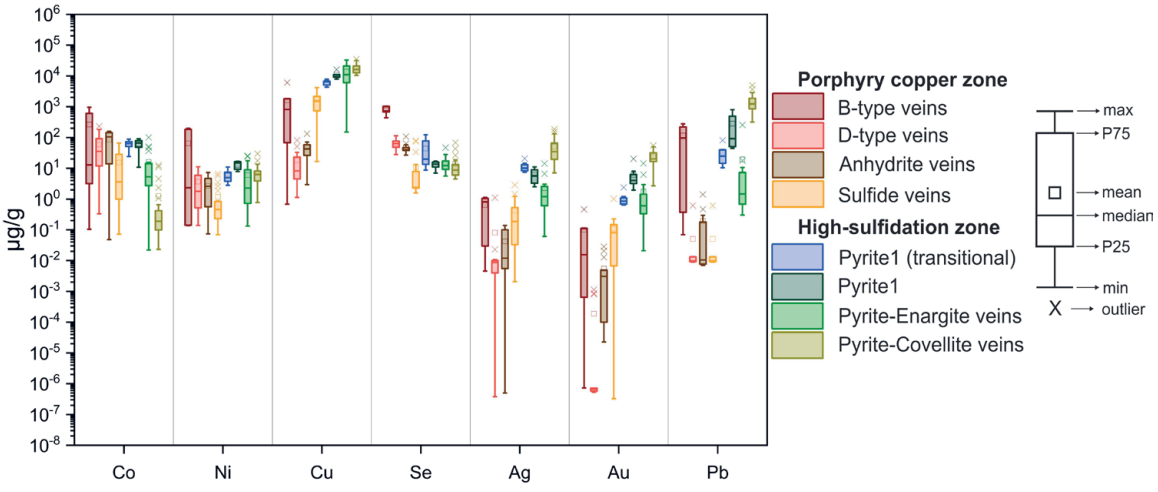

Figure 7. Boxplot comparing concentrations of selected elements analyzed in this study. Variation between vein-types from each ore zone is clearly visible. Note: Below detection limits have been replaced by half of the measurement's individual detection limit, to enable representation of low values. See Table 2. for detection limits.

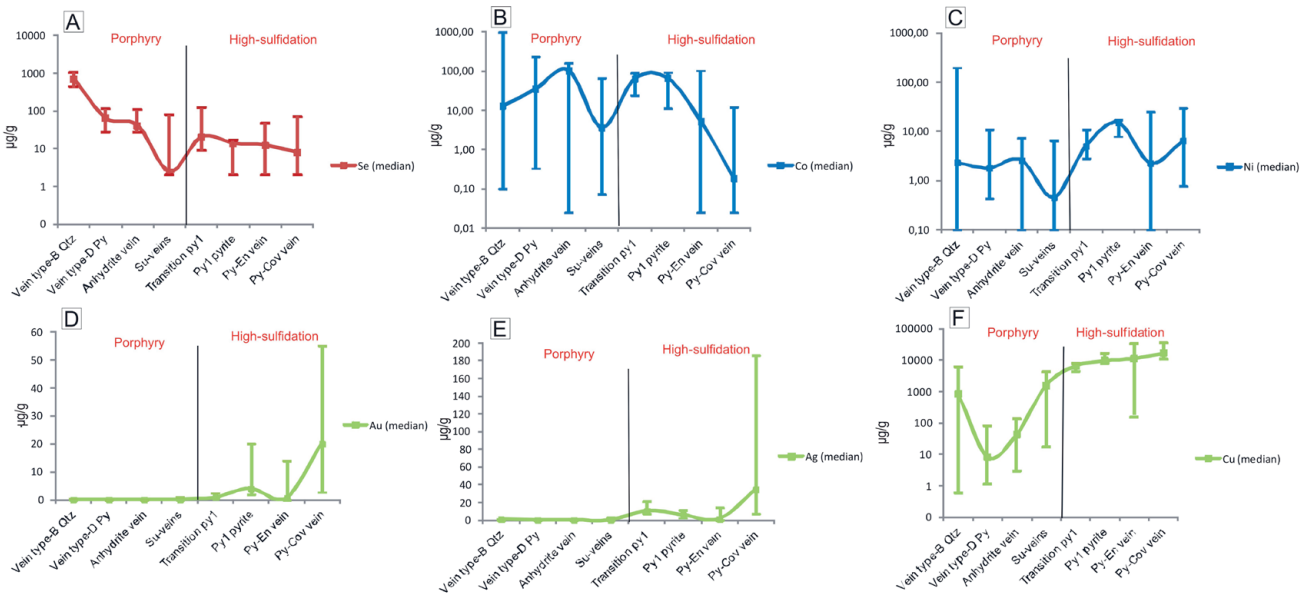

Figure 8. Median values of trace element concentration trends in pyrite from different mineralization zones in Čukaru Peki. The elements that are enriched in pyrite from the porphyry zone are coloured red, those that concentrate around the transition zone are coloured blue, whereas elements enriched in the high-sulfidation zone are coloured green. A) Se concentrations in pyrite have a decreasing trend from the porphyry to epithermal stages; B) Co tends to concentrate in pyrite from anhydrite-veins and in pyrite from the transition zone; C) Ni is enriched in Py1 pyrite, both from the transition zone and high-sulfidation zone ; D) Au concentrations increase rapidly in pyrite from high-sulfidation stage; E) Ag is also significantly enriched in pyrite from the high-sulfidation stage; F) Cu concentrations exhibit a steady increase in pyrite from – the porphyry to the epithermal stages.

Čukaru Peki pyrite demonstrates trace element distribution trends similar to pyrite from other porphyry-epithermal copper deposits (SYKORA et al., 2018). Higher-temperature porphyry-stage pyrite is generally poorer in trace elements compared to the later, lower-temperature epithermal-stage pyrite. SYKORA et al.(2018) show that pyrite crystals from the Lihir (Ladolam) Au porphyry-epithermal deposit in Papua New Guinea, which formed during the earlier, higher-temperature porphyry-stage are enriched in Co, Ni and Se, whereas the later, lower-temperature epithermal-stage is characterized by an enrichment in As, Mo, Ag, Sb, Au and Tl in pyrite.

Decreased Cu concentrations in the pyrite from the porphyry zone of Čukaru Peki can be explained by the fact that Cu is usually bound in Cu-bearing sulfides, including chalcopyrite and bornite (KESLER et al., 2002; REICH et al, 2013). Several studies demonstrate that Cu concentrations in pyrite are very low in the first stages of the porphyry deposits and then gradually increase in the subsequent stages (MAYDAGÁN,et al., 2013; TAN et al., 2021) and are especially elevated in high-sulfidation pyrite (FRANCHINI et al.,2015; SYKORA et al.,2018).

Selenium concentrations in high-sulfidation pyrite that are lower than in the porphyry pyrite at Čukaru Peki are unusual, as Se is typically higher in high-sulfidation pyrite (KEITH et al.,2018; and references therein), although their data does show certain overlaps in pyrite Se concentrations from porphyry to high-sulfidation deposits. Anomalously low Se concentrations in pyrite can be explained by the presence of mineral phases with preferred partitioning of Se, such as selenides, galena or even chalcopyrite (KEITH et al., 2018; PASS, 2010). Selenium concentrations in chalcopyrite have not previously been investigated. Lead-selenides (clausthalite) have solely been identified within the B-type vein of the porphyry ore zone at Čukaru Peki (Fig. 6a). However, time-resolved count signals of pyrite from the significantly Se-enriched B-type veins are smooth and suggest that Se is hosted in the pyrite crystal lattice (or as nanoinclusions) rather than microinclusions of clausthalite. Thus, it seems that the fluids responsible for the formation of B-type veins were significantly Se-enriched, bearing both Se-rich pyrite and clausthalite. Other examples of pyrite from porphyry deposits with elevated Se concentrations have been described, such as a porphyry Cu deposit in the Romanian Metaliferi Mountains (CIOACĂ et al., 2014).

Gold preferably precipitates from the hydrothermal fluids under lower temperature conditions within the epithermal zone, rather than under porphyry higher temperature conditions (e.g. DEDITIUS et al., 2014; SIMMONS, 2005; SYKORA et al., 2018). This is the same trend as observed in Čukaru Peki pyrite. Pyrite from the Čukaru Peki porphyry zone has a median Au concentration of 0.013 µg/g, with a third of the measurements falling below detection limits, compared to the median of 7.2 µg/g Au in the high-sulfidation zone. Decreased concentrations of Au and Ag in pyrite from the porphyry zone of Čukaru Peki can also be explained by the tendency of gold and silver to mainly concentrate in chalcopyrite and bornite in porphyry systems (KESLER et al., 2002; COOK et al., 2011; ZWAHLEN et al., 2014). Also, native Au and electrum are relatively common accessory minerals in these systems (JOHN et al.,2010; SILLITOE, 2010). These accessory minerals are also observed in Čukaru Peki, as demonstrated in Fig.6b, which implies that Au and Ag preferably formed native minerals in this system, instead of being incorporated in pyrite. Recent studies have demonstrated that As-rich pyrite in porphyry systems can concentrate up to 800 ppm Au (REICH et al., 2013; CIOACĂ et al.,2014), but this type of pyrite was not observed in the porphyry zone of Čukaru Peki.

Cobalt-nickel values correspond to pyrite of volcanic origin, according to CAMPBELL & ETHIER (1984). Čukaru Peki pyrite has cobalt concentrations between <1 and <200 µg/g, along with Ni values of maximum 20 µg/g. These low Co-Ni concentrations are in agreement with other studies on pyrite trace element geochemistry (e.g. DEDITIUS et al., 2014; FRANCHINI et

al., 2015; PASS, 2010; REICH et al., 2013), where Co and Ni concentrations range from tens to a few hundreds of µg/g. This suggests that porphyry pyrite predominately has hydrothermal trace element signatures, but may display inherited magmatic trends originating from the magmatic source of the mineralizing hydrothermal fluids.

5.3. Indications of a poly-stage mineralizing fluid evolution by trace element geochemistry

Porphyry–high-sulfidation systems form by multiple pulses of hydrothermal fluids circulating through the overlying host rock, driven by underlying intrusions (SILLITOE, 2010; INGEBRITSEN & APPOLD, 2012). Pyrite in these systems commonly exhibits zoning associated with polyphase fluid evolution (SYKORA et al., 2018) and may thus have zones with trace element compositions related to the different phases of hydrothermal fluids (FRANCHINI et al., 2015).

The epithermal stage in the evolution of porphyry systems is characterized by high-, intermediate- or low-sulfidation veins (and alteration) that form under lower temperatures and salinities than earlier porphyry veins (JOHN et al., 2010; SILLITOE, 2010). In these later stages, hydrothermal events that overprint the porphyry-style ore commonly remobilize Cu and Au, since the original chalcopyrite-bornite minerals are dissolved. In this way, Au and Cu are introduced into epithermal systems (KESLER et al., 2002; REICH et al., 2013; GREGORY et al., 2013). This process is particularly interesting in high-sulfidation deposits, since they are genetically and spatially associated with underlying porphyry systems (KESLER et al., 2002; SILLITOE, 2010). In many high-sulfidation systems, pyrite commonly contains invisible gold in the crystal lattice (CHOUINARD et al., 2005; BOGDANOV & KUNCHEVA, 2017), but in some cases it also contains significant amounts of crystal lattice-bound Cu (PAČEVSKI et al.,2008). POKROVSKI et al. (2019) argue that chemisorption is the most common process in which invisible gold is incorporated into pyrite as Au(I) ions.

In Čukaru Peki, the polyphase genesis is evident from multiple generations of veins (Tables 3 and 4; Fig.5). The process of primary sulfide dissolution can be observed in the transition zone of Čukaru Peki, where covellite and enargite replace the primary mineralization of chalcopyrite and bornite. Significantly elevated concentrations of elements are attributed to the high-sulfidation zone (e.g. Cu, Ag, Cd, In, Sn, Pb and Bi). Five spot measurements of the porphyry zone pyrite crystals (B-type veins and Purple anhydrite-veins) suggest that these veins were affected by later high-sulfidation fluids. The later fluids could have resulted in pyrite growth zones that would be enriched in these high-sulfidation associated elements. Elevated Cd is particularly interesting, as Cd is only seen above detection limits in the pyrite-covellite veins, which represent the latest veins investigated in this study. This could indicate that the later hydrothermal fluids, responsible for the pyrite-covellite veins, originated from the deeper parts of the hydrothermal system. An additional argument for this statement is the apparent compositional similarity between sulfide-veins (Fig.5.h), which are found in the porphyry and transitional zones and pyrite-covellite veins (Fig.5c) which are found in the high-sulfidation zone. Both of these veins contain abundant covellite, which is a common mineral for the high-sulfidation zone, but uncommon for porphyry conditions (JOHN et al., 2010; SILLITOE, 2010). This suggests that sulfide-veins formed by the same or similar fluids that led to the remobilization of primary sulfides and redeposition in the high-sulfidation zone. Pyrite from sulfide-veins differs from pyrite from py-cov veins, both in its textural characteristics (lack of colloform texture) and in its trace element composition (depleted concentrations of Au, Ag and Cu). However, this can possibly be explained by the different temperatures at which these two vein types were formed, which probably affected the depositional textures and element distributions.

DURAN et al. (2019) investigated pyrite trace element compositions from a range of deposit types (VMS, orogenic Au, porphyry Cu and magmatic). Based on this, DURAN et al. (2019) were able to distinguish pyrite from hydrothermal and magmatic origins based on their Co/Sb and Se/As variations (Fig. 9). Čukaru Peki pyrite from the porphyry zone (and transition zone) plot predominantly within the magmatic zone (marked with an orange colour), with overlaps into the hydrothermal zone , which is the case for the porphyry Cu field in the DURAN et al. (2019) diagram. High-sulfidation zone (marked with a green colour) pyrite plots well within the hydrothermal domain proposed by DURAN et al. (2019). This is reasonable as the fluids responsible for the porphyry zone, especially, would have a significant magmatic signature. This is further demonstrated with fluid inclusion analyses by VELOJIĆ et al. (2020). Earlier and deeper porphyry zone veins, such as the B-type veins, show a more magmatic signature

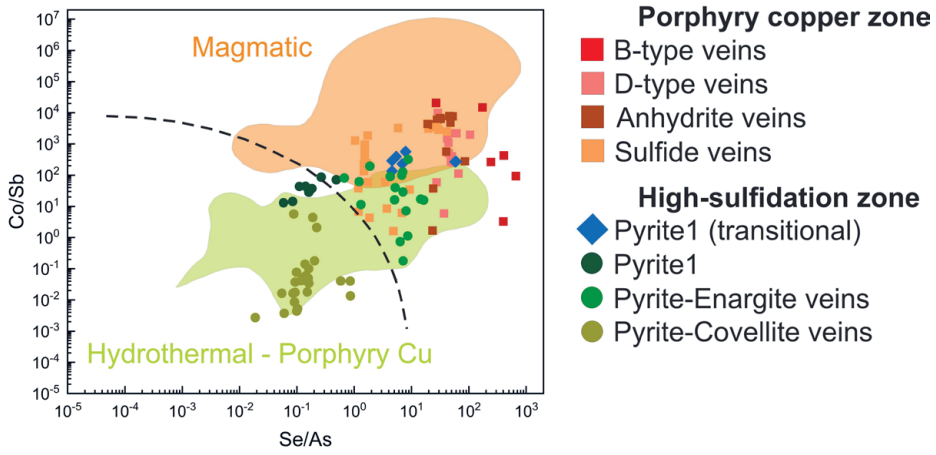

Figure 9. Discrimination plot for pyrite formed from hydrothermal or magmatic origins (indicated by the dashed line), based off Se/As vs Co/Sb values. Two domains are drawn out, based on where the porphyry and magmatic pyrite data clusters. Plot and domains are made after DURAN et al. (2019). Note: Below detection limits have been replaced by half of the measurement's individual detection limit, to enable representation of low values. See Table 2. for the detection limits.

with homogenization temperatures between 331 and 495ºC and salinities between 36.5 and 43 wt% NaCl eq, whereas anhydrite veins were formed by fluids with significantly lower salinities. It is important to note that porphyry zone pyrite would not be expected to plot perfectly within the magmatic domain, as they are still the product of hydrothermal fluids. Rather, the hydrothermal fluids responsible for the mineralization display a slight magmatic signature, inherited from the magmatic source. These pyrites were not formed in the magma itself and thus do not show a true magmatic signature.

6. CONCLUSIONS

The results obtained demonstrate that the different veins in Čukaru Peki can be distinguished by both their mineralogy and trace element compositions. The porphyry zone pyrite crystals generally contain lower concentrations of most trace elements and are only significantly enriched in Co and Se. Transition pyrite mostly shows trace element concentrations between the two other zones, having lower concentrations more similar to pyrite from the porphyry zone. High-sulfidation pyrite crystals are characterized by enrichment of V, Mn, Ni, Cu, As, Mo, Ag, Cd, In, Sn, Sb, Au, Hg, Tl, Pb and Bi. Increased concentrations of elements attributed to the high-sulfidation zone in five spot measurements of the porphyry zone pyrites crystals from Quartz veins type B and purple anhydrite veins imply that these veins were affected by later high-sulfidation fluids. However, there are many differences in trace element concentrations between the different pyrite crystals of each zone.

The ore-microscopic and SEM studies imply that the most important stage for the deposition of Cu and Au in the porphyry system was quartz veins type B. These veins contain the highest amounts of Cu-bearing sulfides (chalcopyrite and bornite). Additionally, SEM studies have demonstrated the presence of native Au and electrum grains in these veins (Fig.6b and 6d). Concentrations of Au and Ag in pyrite are low, which indicates that these two elements formed native minerals (native Au and electrum) or were partitioned into chalcopyrite or bornite. Another important type of vein for Cu deposition are the sulfide veins, which contain abundant covellite and probably represent the transition to the epithermal stage of mineralization.

According to the ore-microscopic research and LA-ICP-MS measurements, we conclude that the most important stage for the deposition of Cu and Au in the high-sulfidation zone are the pyrite-covellite (py-cov) veins. They contain the highest amounts of Cu-sulfides (covellite and enargite) as well as the highest concentrations of Au and Ag in the analyzed pyrite grains. Pyrite-enargite veins also contain abundant enargite, but much less covellite than the pyrite-covellite veins, thus they have lower Cu contents. However, it should be noted that preliminary measurements indicate that enargite from pyrite-enargite veins contains elevated concentrations of germanium (VELOJIĆ & ERLANDSSON, 2019).

Our pyrite trace element data illustrates the change in mineralizing hydrothermal fluids; from a magmatic-sourced system (the porphyry zone) to a more typical hydrothermal system that was responsible for the high-sulfidation zone mineralization. There is also evidence for the late high-sulfidation fluids affecting the earliest and deeper pyrite in the porphyry zone, by growth of pyrite enriched in elements characteristic of the high-sulfidation mineralization.

It is established that the main gold-concentrating mineral in this zone is pyrite, which is commonly not considered an ore mineral during mineral processing and thus it is usually not included in the main sulfide concentrate. The results presented might also be significant for the better targeting of specific gold- and silver-rich veins and mineralization stages during mineral exploration.

ACKNOWLEDGEMENT

This contribution is supported by the project "rESEErve - Mineral potential of the ESEE region" funded by the European Institute of Innovation and Technology (EIT), a body of European Union, under the Horizon 2020, the EU Framework Programme for Research and Innovation.

The authors would like to thank the geologists from the Rakita Exploration Company for their assistance in sampling and geological interpretation (now called Balkan Expploration and Mining). This research was partly funded with an Ernst Mach Grant by OEAD agency and with Ceepus mobility grant. Two anonymous reviewers and the editor are thanked for their constructive comments in improving the manuscript.

REFERENCES

BANJEŠEVIĆ, M. & LARGE, D. (2014): Geology and mineralization of the new copper and gold discovery south of Bor Timok magmatic complex.– In: Proceedings of the XVI Serbian Geological Congress, Serbian Geological Society, Donji Milanovac, 2014, 739–741.

BANJEŠEVIĆ, M., CVETKOVIĆ, V., VON QUADT, A., LJUBOVIĆ OBRADOVIĆ, D., VASIĆ, N., PAČEVSKI, A. & PEYTCHEVA, I. (2019): New Constraints on the Main Mineralization Event Inferred from the Latest Discoveries in the Bor Metallogenetic Zone (BMZ, East Serbia).– Minerals, 9/11, 672. https://doi.org/10.3390/min9110672

BOGDANOV, K., & KUNCHEVA, J. (2017): Epithermal gold mineralization in the Krassen deposit, Panagyurishte ore district, Bulgaria.– Geologica Macedonica, 31/2, 107–116.

CAMPBELL, F.A. & ETHIER, V.G. (1984): Nickel and cobalt in pyrrhotite and pyrite from the Faro and Sullivan ore bodies.– The Canadian Mineralogist, 22, 503–506.

CHOUINARD, A., PAQUETTE, J. & WILLIAMS-JONES, A.E. (2005): Crystallographic controls on trace-element incorporation in auriferous pyrite from the Pascua epithermal high-sulfidation deposit, Chile–Argentina.– The Canadian Mineralogist, 43/3, 951–963. doi: 10.2113/gscanmin.43.3.951

CIOACĂ, M.E., MUNTEANU, M., QI, L. & COSTIN, G. (2014): Trace element concentrations in porphyry copper deposits from Metaliferi Mountains, Romania: A reconnaissance study.– Ore Geology Reviews, 63, 22–39. doi: 10.1016/j.oregeorev.2014.04.016

COOK, N.J., CIOBANU, C.L., DANYUSHEVSKY, L.V. & GILBERT, S. (2011): Minor and trace elements in bornite and associated Cu–(Fe)-sulfides: A LA-ICP-MS study Bornite mineral chemistry.– Geochimica et Cosmochimica Acta, 75/21, 6473–6496. doi: 10.1016/j.gca.2011.08.021

DEDITIUS, A.P., REICH, M., KESLER, S.E., UTSUNOMIYA, S., CHRYSSOULIS, S.L., WALSHE, J. & EWING, R.C. (2014): The coupled geochemistry of Au and As in pyrite from hydrothermal ore deposits.– Geochimica et Cosmochimica Acta, 140, 644–670. doi: 10.1016/j.gca.2014.05.045

DROVENIK, M. (1961): Geological-petrological study of the Bor mine area (eastern Serbia) (in Slovenian).– Unpubl. PhD Theses, Ljubljana, 344 p.

DURAN, C.J., DUBÉ-LOUBERT, H., PAGÉ, P., BARNES, S.-J., ROY, M., SAVARD, D. CAVE, B.J., ARGUIN, J.-P. & MANSUR, E.T. (2019): Applications of trace element chemistry of pyrite and chalcopyrite in glacial sediments to mineral exploration targeting: Example from the Churchill Province, northern Quebec,– Canada Journal of Geochemical Exploration, 196, 105–130. doi: 10.1016/j.gexplo.2018.10.006

FRANCHINI, M., MCFARLANE, C., MAYDAGÁN, L., REICH, M., LENTZ, D.R., MEINERT, L. & BOUHIER, V. (2015): Trace metals in pyrite and marcasite from the Agua Rica porphyry-high sulfidation epithermal deposit, Catamarca, Argentina: Textural features and metal zoning at the porphyry to epithermal transition.– Ore Geology Reviews, 66, 366–387. doi: 10.1016/j.oregeorev.2014.10.022

FÜGENSCHUH, B. & SCHMID, S.M. (2005): Age and significance of core complex formation in a very curved orogen: Evidence from fission track studies in the South Carpathians (Romania).– Tectonophysics, 404/1–2, 33–53. doi: 10.1016/j.tecto.2005.03.019

GALLHOFER, D., QUADT, A. V., PEYTCHEVA, I., SCHMID, S. M., & HEINRICH, C.A. (2015): Tectonic, magmatic, and metallogenic evolution of the Late Cretaceous arc in the Carpathian-Balkan orogen.– Tectonics, 34/9, 1813–1836. doi: 10.1002/2015TC003834

GREGORY, M.J., LANG, J.R., GILBERT, S. & HOAL, K.O. (2013): Geometallurgy of the Pebble porphyry copper-gold-molybdenum deposit, Alaska: Implications for gold distribution and paragenesis.– Economic Geology, 108/3, 463–482. doi: 10.2113/econgeo.108.3.463

INGEBRITSEN, S.E. & APPOLD, M.S. (2012): The physical hydrogeology of ore deposits.– Economic Geology, 107/4, 559–584. doi: 10.2113/econgeo.107.4.559

JAKUBEC, J., MACSPORRAN, G., DUINKER, P., PITTUCK, M., MANOLJOVIĆ, P., SUCHARDA, M., SAMOUKOVIĆ, M., BUNYARD, C. & ARSENEAU, G. (2018): NI 43-101 Technical Report-Timok Copper-Gold Project, Serbia: Upper Zone Prefeasibility Study and Resource Estimate for the Lower Zone.– Nevsun Resources Ltd, 1–427.

JANKOVIĆ, S. (1990): The ore deposits of Serbia (Yugoslavia): Regional metallogenic setting, enviroments of deposition and types (in Serbian, with english summary).– Faculty of Mining and Geology, Belgrade, 760 p.

JANKOVIĆ, S., JELENKOVIĆ, R. & KOŽELJ, D. (2002): The Bor copper and gold mine.– QWERTY, Bor, 298 p.

JELENKOVIĆ, R., MILOVANOVIĆ, D., KOŽELJ, D. & BANJEŠEVIĆ, M. (2016): The mineral resources of the Bor metallogenic zone: a review.– Geologia Croatica, 69/1, 143–155. doi: 10.4154/GC.2016.11

JOHN, D.A., AYUSO, R.A., BARTON, M.D., BLAKELY, R.J., BODNAR, R.J., DILLES, J.H., GRAY, F., GRAYBEAL, F.T., MARS, J.L., McPHEE, D., SEAL, R.R. & TAYLOR, R.D. (2010): Porphyry copper deposit model.– Scientific investigations report. doi: 10.3133/sir20105070B

KEITH, M., SMITH, D.J., JENKIN, G.R.T., HOLWELL, D.A. & DYE, M.D. (2018): A review of Te and Se systematics in hydrothermal pyrite from precious metal deposits: Insights into ore-forming processes.– Ore Geology Reviews, 96, 269–282. doi: 10.1016/j.oregeorev.2017.07.023

KESLER, S.E., CHRYSSOULIS, S.L. & SIMON, G. (2002): Gold in porphyry copper deposits: its abundance and fate.– Ore Geology Reviews, 21/1–2, 103–124. doi: 10.1016/S0169-1368(02)00084-7

KNAAK, M., MÁRTON, I., TOSDAL, R. M., VAN DER TOORN, J., DAVIDOVIC, D., STRMBANOVIC, I. & HASSON, S. (2016): Geologic setting and tectonic evolution of porphyry Cu-Au, polymetallic replacement, and sedimentary rock-hosted au deposits in the northwestern area of the Timok magmatic complex, Serbia.– Serbia, Society of Economic Geologists, Special Publication, 19, 1–28.

KOLB, M., VON QUADT, A., PEYTCHEVA, I., HEINRICH, C.A., FOWLER, S.J. & CVETKOVIĆ, V. (2013): Adakite-like and normal arc magmas: distinct fractionation paths in the East Serbian segment of the Balkan–Carpathian arc.– Journal of Petrology, 54/3, 421–451. doi: 10.1093/petrology/egs072

MAYDAGÁN, L., FRANCHINI, M., LENTZ, D., PONS, J. & MCFARLANE, C. (2013): Sulfide composition and isotopic signature of the Altar Cu-Au deposit, Argentina: Constraints on the evolution of the porphyry-epithermal system.– The Canadian Mineralogist, 51/6, 813–840. doi: 10.3749/canmin.51.6.813

MIŠKOVIĆ, V. (1989): The genesis of copper deposit "Novo Okno" and its metallogenic corellation with ore clasts in Bor region- eastern Serbia (in Serbian).– Unpubl. PhD Theses, Faculty of Mining and Geology, Belgrade, 189 p.

NEUBAUER, F. (2002): Contrasting Late Cretaceous with Neogene ore provinces in the Alpine-Balkan-Carpathian-Dinaride collision belt.– Geological Society London Special Publication, 204, 90–100. doi: 10.1144/GSL.SP.2002.204.01.06

ONUK, P., MELCHER, F., MERTZ-KRAUS, R., GÄBLER, H.E. & GOLDMANN, S. (2017): Development of a matrix-matched sphalerite reference material (MUL-ZnS-1) for calibration of in situ trace element measurements by laser ablation-inductively coupled plasma-mass spectrometry.– Geostandards and Geoanalytical Research, 41/2, 263–272. doi: 10.1111/ggr.12154

PAČEVSKI, A., LIBOWITZKY, E., ŽIVKOVIĆ, P., DIMITRIJEVIĆ, R. & CVETKOVIĆ, L. (2008): Copper-bearing pyrite from the Čoka Marin polymetallic deposit, Serbia: Mineral inclusions or true solid-solution?.– The Canadian Mineralogist, 46/1, 249–261. doi: 10.3749/canmin.46.1.249

PAČEVSKI, A., CVETKOVIĆ, V., ŠARIĆ, K., BANJEŠEVĆ, M., HOEFER, H.E. & KREMENOVIĆ, A. (2016): Manganese mineralization in andesites of Brestovačka Banja, Serbia: evidence of sea-floor exhalations in the Timok Magmatic Complex.- Mineralogy and Petrology, 110/4, 491. doi: 10.1007/s00710-016-0425-7

PASS, H.E. (2010): Breccia-hosted chemical and mineralogical zonation patterns of the Northeast Zone, Mt. Polley Cu-Ag-Au alkalic porphyry deposit, British Columbia, Canada.– PhD thesis, University of Tasmania.

PATON, C., HELLSTROM, J., PAUL, B., WOODHEAD, J. & HERGT, J. (2011): Iolite: Freeware for the visualisation and processing of mass spectrometric data.– Journal of Analytical Atomic Spectrometry. doi:10.1039/c1ja10172b.

PAVIĆEVIĆ, M., RAKIĆ, S., GRŽETIĆ, I. & GOLIJANIN, D. (1981): A study of distribution of precious, rare and trace elements in the ore body "Tilva Roš" in Bor mine (in Serbian).– Faculty of Mining and Geology ULEMA, Belgrade, 102 p.

PAVIĆEVIĆ, M., RAKIĆ, S., GRŽETIĆ, I. & GOLIJANIN, D. (1985): A study of distribution of precious, rare and trace elements in the Borska reka ore deposit (in Serbian).– Faculty of Mining and Geology ULEMA, Belgrade, 112 p.

POKROVSKI, G.S., KOKH, M.A., PROUX, O., HAZEMANN, J.L., BAZARKINA, E.F., TESTEMALE, D., ... & THIBAUT, M. (2019): The nature and partitioning of invisible gold in the pyrite-fluid system.– Ore Geology Reviews, 109, 545–563. doi: 10.1016/j.oregeorev.2019.04.024

REICH, M., DEDITIUS, A., CHRYSSOULIS, S., LI, J. W., MA, C.Q., PARADA, M.A., ... & MITTERMAYR, F. (2013): Pyrite as a record of hydrothermal fluid evolution in a porphyry copper system: A SIMS/EMPA trace element study.– Geochimica et Cosmochimica Acta, 104, 42–62. doi: 10.1016/j.gca.2012.11.006

SILLITOE, R.H. (2010): Porphyry copper systems.– Economic geology, 105/1, 3–41. doi: 10.2113/gsecongeo.105.1.3

SIMMONS, S.F. (2005): Geological characteristics of epithermal precious and base metal deposits.– In: 100th Anniversary Volume, 485–522. doi: 10.5382/AV100.16

SYKORA, S., COOKE, D. R., MEFFRE, S., STEPHANOV, A. S., GARDNER, K., SCOTT, R., ... & HARRIS, A.C. (2018): Evolution of pyrite trace element compositions from porphyry-style and epithermal conditions at the Lihir gold deposit: Implications for ore genesis and mineral processing.– Economic Geology, 113/1, 193–208. doi: 10.5382/econgeo.2018.4548

VAKANJAC, B. (2000): A comparative study of typical paragenetic relations in different ore of Bor metallogenic zone (in Serbian)– Doctoral dissertation, Faculty of Mining and Geology, Belgrade, 314 p.

VELOJIĆ, M. & BERTRANDSSON ERLANDSSON, V. (2019): Trace elements in different veins by LA-ICP-MS in Chukaru Peki high sulfidation deposit, Serbia.– In: 1st International Student Conference on Geochemistry and Mineral Deposits, Prague.

VELOJIĆ, M., JELENKOVIC, R. & CVETKOVIC, V. (2020): Fluid Evolution of the Čukaru Peki Cu-Au Porphyry System (East Serbia) inferred from a fluid inclusion study.– Geologia Croatica, 73/3, 197–209. doi: 10.4154/gc.2020.14

VON QUADT, A. PEYTCHEVA, I., CVETKOVIĆ, V. BANJEŠEVIĆ, M. & KOŽELJ, D. (2002): Geochronology, geochemistry and isotope tracing of the Cretaceous magmatism of East-Serbia as part of the Apuseni-Timok-Srednogorie metallogenic belt.– Geologica Carpathica, 53, 175–177.

WILSON, S.A., RIDLEY, W.I. & KOENIG, A.E. (2002): Development of sulfide calibration standards for the laser ablation inductively-coupled plasma mass spectrometry technique.– International Journal of Analytical Atomic Spectrometry, 17, 406–409. doi: 10.1039/B108787H

ZWAHLEN, C., CIOLDI, S., WAGNER, T., REY, R. & HEINRICH, C. (2014): The porphyry Cu-(Mo-Au) deposit at Altar (Argentina): Tracing gold distribution by vein mapping and LA-ICP-MS mineral analysis.– Economic Geology, 109/5, 1341–1358. doi: 10.2113/econgeo.109.5.1341

Geologia Croatica